Soil moisture drydown curves after flooding events across an irrigated farmland

Gaxiola-Ortiz F[1]., Álvarez-Yepiz J. C. [1], Franz T. [2], Garatuza-Payan J. [1], Guevara M.[3], Peñuelas-Rubio O. [4], Rosolem R. [5], Torres-Velázquez J. R. [4], Yepez E. A. [1], Sanchez-Mejia Z. [1]

[1] Instituto Tecnológico de Sonora, Ciudad Obregón, Sonora, México [2] University of Nebraska-Lincoln, Lincoln, NE, USA [3] Universidad Nacional Autónoma de México, Juriquilla, Querétaro, México [4] Instituto Tecnológico del Valle del Yaqui, Bácum, Sonora, México [5] University of Bristol, Bristol, UK

corresponding author: francisco.gaxiola111644@potros.itson.edu.mx and zulia.sanchez@itson.edu.mx

1. Introduction

Soil moisture (θ) is a key variable for agriculture, however θ monitoring has gaps at intermediate scales which makes decision making challenging at field scale. Therefore, technology like cosmic-ray neutron sensors (CRNS) and time domain reflectometry (TDR) provide a unique research opportunity. An approach to analyze time series of θ observations is through drydown curves. After an irrigation event, θ decreases gradually with time, the rate (cm³/ cm³ / day) at which θ decreases is called θ_{decay}. When the remaining θ is 1/3 of the initial θ we reach the $\theta_{threshold}$, which could be close to the wilting point and may be an indicator of dryness. Better understanding θ_{decay} and $\theta_{threshold}$ can provide insight for water management purposes.

2. Objective and hypothesis

O1. Characterize the θ through the use of drydown curves and the $\theta_{threshold}$, at each irrigation event for the winter wheat crop year 2019-2020.
O2. Quantify the impact of meteorological conditions and vegetative greenness in θ after every irrigation event.

H1. Drydown curves and $\theta_{threshold}$ will be different after every irrigation event and between observation methods due to spatial scale.
H2. Meteorological variables correlated with θ will be different with every irrigation event.

3. Materials and methods

- Study site: Yaqui Valley, Sonora, México (Fig. 1 a).
- Crop: Wheat (*Triticum spp.*).
- Cycle 2019 – 2020: Mid-December to Late-April.
- Crop phenology proxy – NDVI (Landsat 8 USGS/Google Engine).
- Drydown curve (Sanchez-Mejia and Papuga, 2014) (Fig. 1 c).
- Multivariate statistical analysis.

- 1 TDR$_{profile}$ in Vegetated (ridge) and 1 TDR$_{profile}$ in Bare Soil (furrow) (Fig. 1 b).
- CRNS Calibration (Desilets et al., 2010; Rosolem et al 2013) (Fig. 1 b).

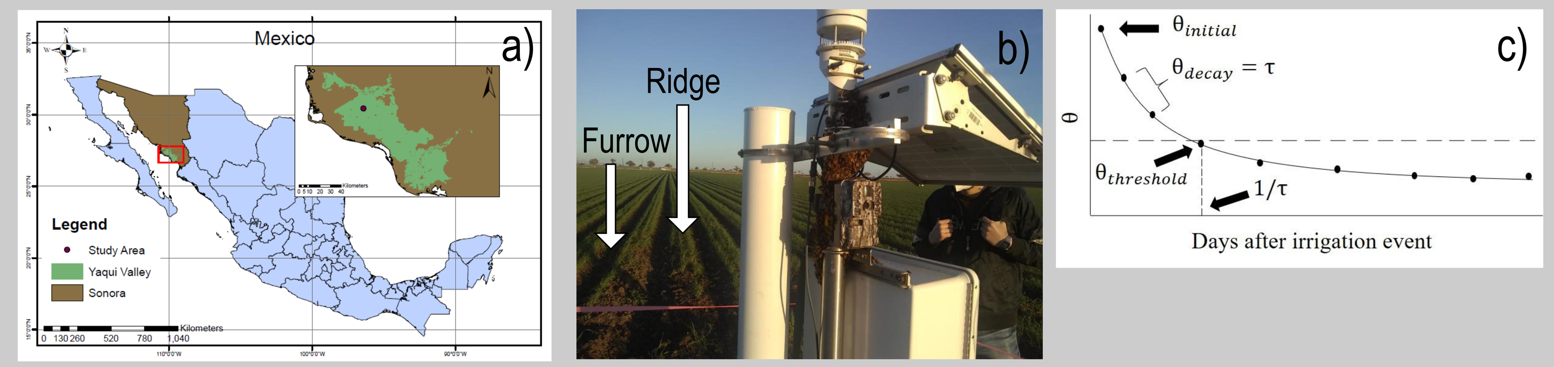

Fig. 1 a) Yaqui Valley (240,000 ha) agriculture footprint in NW México, b) Main crop winter wheat with flood irrigation and CRNS (Hydroinnova®), weather sensor (ClimaVUE™ 50, Campbell Scientific®), soil profilers (TDRs, SoilVUE™ 10, Campbell Scientific®) and radiometer (4-WR, Apogee Instruments®) and c) Conceptual diagram of a drydown curve, θ_{decay}, $\theta_{threshold}$ and time to reach threshold ($1/\tau$).

A detailed set of equations can be found scanning the QR-code

Drydown analysis was performed for each irrigation event, from the day of irrigation ($\theta_{initial}$) to the day before the next irrigation. The exponential model in equation 1 was fit to obtain θ_{decay} and $\theta_{threshold}$.

$$\theta(t) = (\theta_i - \theta_f)e^{(-t/\tau)} + \theta_f \qquad \text{(eq 1)}$$

Where θ is the volumetric soil moisture (cm³/cm³), t is the time in days after the irrigation event, θ_i is the soil moisture on the first day of the irrigation event (cm³/cm³), θ_f is the soil moisture on the last day of the drydown curve (cm³/cm³) and τ is the exponential time constant.

τ represents the value of θ_{decay} and at time ($1/\tau$) we have our $\theta_{threshold}$ which represents 1/3 of the moisture left (Fig. 1 c).

4. Soil moisture time series, decay, and threshold

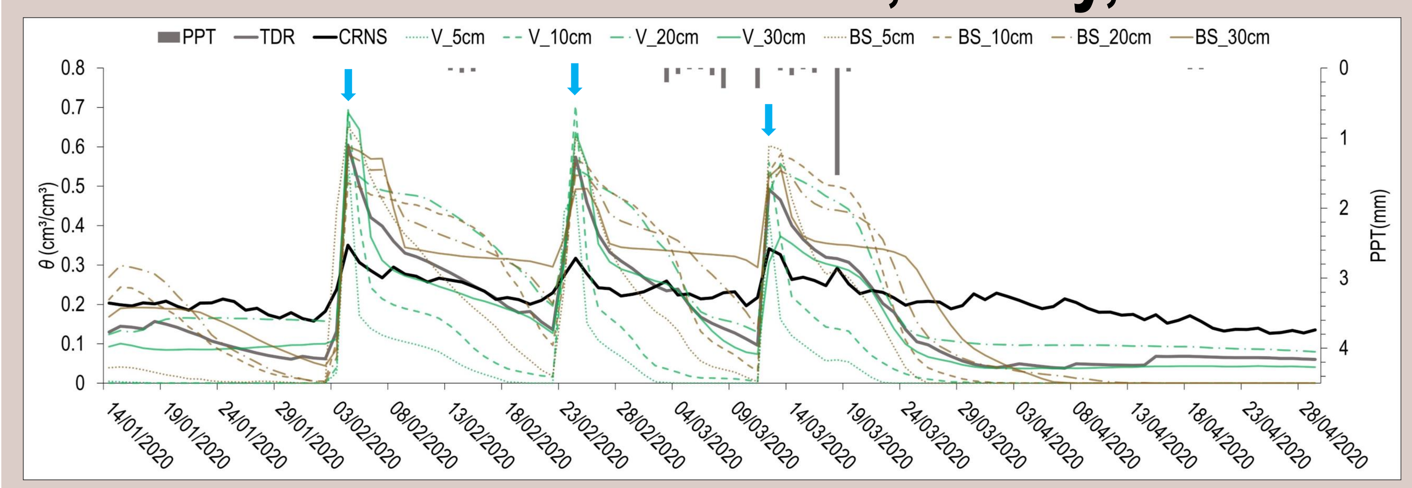

Fig. 2 Time series of θ from CRNS, 2 TDR (5, 10, 20 and 30 cm depth), TDR integrated (averaged 5-30 cm) and precipitation (PPT). Blue arrows indicate irrigation events.

- TDR: sensible to irrigations and PPT (> 2 cm) (Fig. 2).
- CRNS: sensible to irrigations and PPT (> 0.5 cm).
- Different spatial scales may explain the different observed magnitudes between CRNS and integrated TDR.

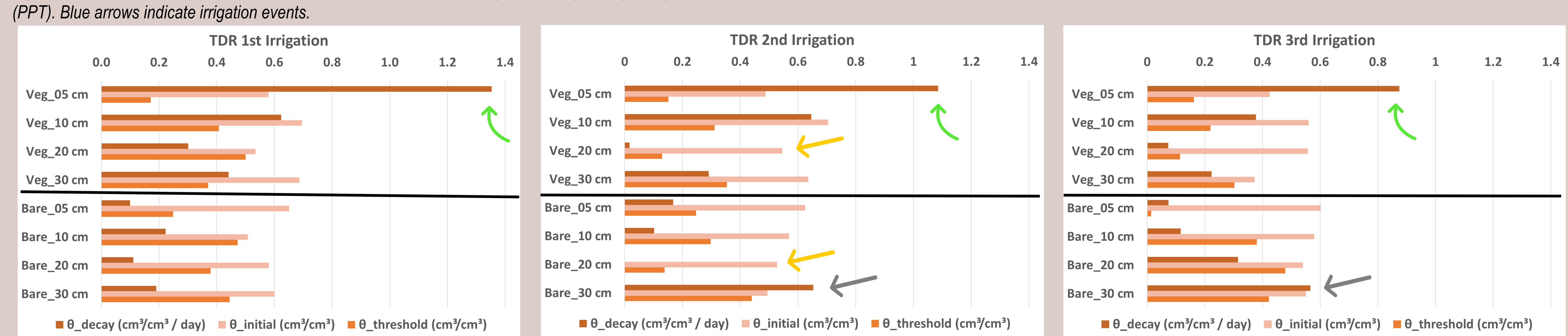

Fig. 3 θ_{decay} and $\theta_{threshold}$ following each irrigation event, from vegetated and bare soil at different depths (5-30 cm).

- θ_{decay} tends to be higher for the vegetation site (ridge) than the bare soil site (furrow) for the 3 irrigations (green arrows) (Fig. 3).
- θ_{decay} is slow at depths beyond 10 cm (yellow arrows), leading to a longer time to dry.
- On average $\theta_{threshold}$ for the bare soil site (0.330 ± 0.145) tends to be higher than vegetation site (0.266 ± 0.126).
- After the 2nd and 3rd irrigation θ_{decay} from deeper layers (30 cm) at the bare soil site increased (gray arrows).

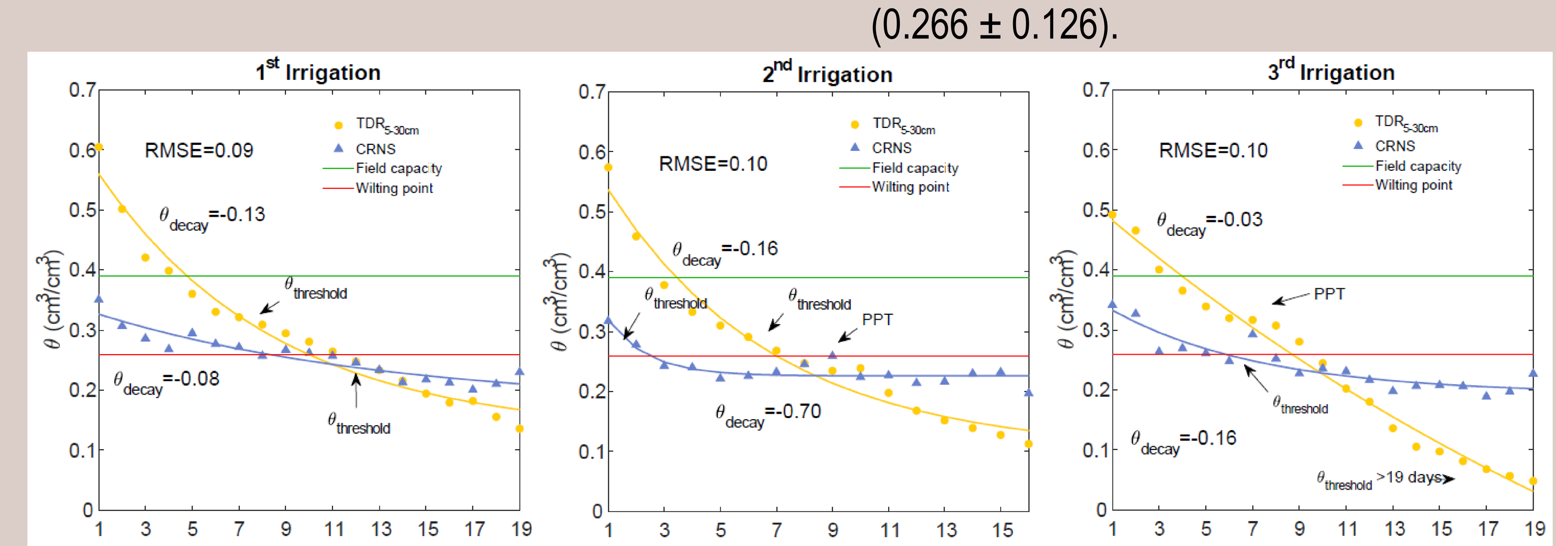

Fig. 4 Drydown curves with θ_{decay} and $\theta_{threshold}$ following each irrigation event, TDR integrated (averaged 5-30 cm) vs CRNS.

- Following irrigation CRNS never presents $\theta_{initial}$ over field capacity, contrary to the TDR (Fig 4).
- θ_{decay} is higher for CRNS after the 2nd and 3rd irrigation event.
- In general, the RMSE for TDR vs CRNS from drydown curves are low despite the spatial difference each sensor overseas.
- θ_{decay}, $\theta_{threshold}$ and the time to reach it are different between TDR and CRNS.

5. Multivariate analysis during θ drydown after irrigation events

Table 1. Spearman correlation coefficient matrix between θ estimated from TDR and CRNS (θ_{TDR} and θ_{CRNS}) with air temperature (T_{air}), soil temperature averaged 5-30 cm (T_{soil}), evapotranspiration (ET), vapor pressure deficit (VPD), normalized difference vegetation index (NDVI), precipitation (PPT), short wave incoming radiation (SW_{in}) and difference between T_{air} and T_{soil} (ΔT).

	1st Irrigation		2nd Irrigation		3rd Irrigation	
	θ_{TDR}	θ_{CRNS}	θ_{TDR}	θ_{CRNS}	θ_{TDR}	θ_{CRNS}
θ_{TDR}	X	0.91	X	0.65	X	0.43
θ_{CRNS}	0.91	X	0.65	X	0.43	X
T_{air}	-0.78	-0.71	-0.35	-0.24	-0.22	-0.61
T_{soil}	-0.65	-0.55	-0.13	0.19	-0.30	-0.74
ET	0.15	-0.06	0.53	0.15	0.71	0.32
VPD	0.05	-0.21	0.62	0.13	-0.28	-0.81
NDVI	-0.30	-0.42	-0.33	-0.24	0.45	0.84
PPT	-0.04	-0.02	-0.53	-0.30	0.51	0.43
SW_{in}	0.24	0.20	0.64	0.27	-0.19	-0.51
ΔT	-0.64	-0.67	-0.48	-0.53	-0.03	0.16

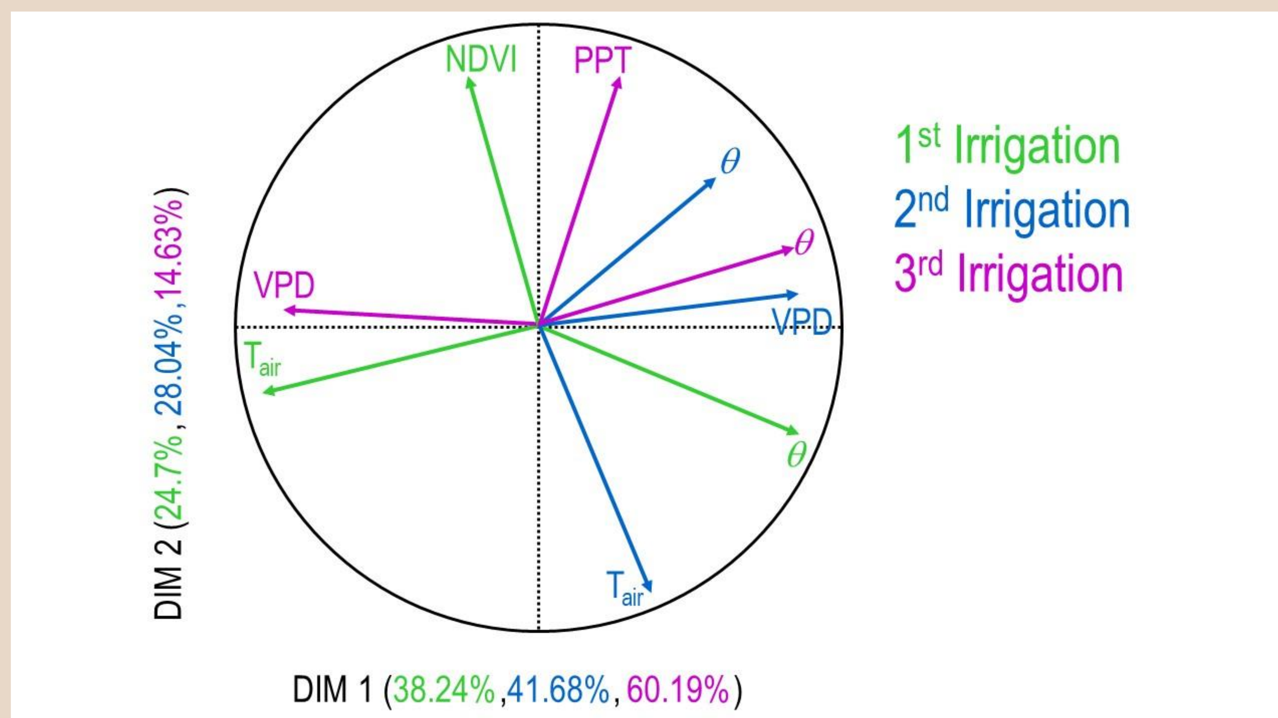

Fig. 5 Principal component analysis (PCA) between θ estimated from TDR (1st and 2nd irrigation) and CRNS (3rd irrigation), air temperature (T_{air}), vapor pressure deficit (VPD), normalized difference vegetation index (NDVI), and precipitation (PPT).

- After each irrigation, the correlation of θ with NDVI and meteorological variables, varied in strength and signal (+/-) (Table 1).
- θ from TDR and CRNS correlates best (r>0.9) during 1st irrigation and least (r~0.4) during the 3rd irrigation, scattering was observed at lower θ values.
- θ is highly (r>0.7) negatively correlated with T_{air} and T_{soil} during 1st irrigation, and with the temperature difference between air and soil.
- ET increases its correlation with θ after every irrigation event.
- VPD (-) and NDVI (+) had a strong correlation (r>0.8) with θ during the 3rd irrigation.

- The variation explained by PC1 and PC2 increased with each irrigation event (63% < 70% < 75%) (Fig 5).
- Variables that best explain PC1 and PC2 change with every irrigation.
- Temperature and θ consistently show and inverse correlation.
- After each irrigation event, VPD and NDVI are inversely correlated.
- Vectors related to θ from TDR and CRNS, started together and became apart with each irrigation.

6. Take home message and future work

- θ_{decay} and $\theta_{threshold}$ values indicate differences at spatial and temporal scales. Higher θ_{decay} was observed in the vegetation site in contrast to the bare soil site; and at the same time, average $\theta_{threshold}$ for bare soil site is higher but with more variation.
- Differences between TDR and CRNS are observable in θ_{decay}, $\theta_{threshold}$, correlations and PCA, which supports the idea of both sensors observing the same at different scales. CRNS could be more suitable for water management at field scale.
- After each irrigation, meteorological variables highly correlated with θ and the variables that better explain PC1 and PC2 changed. Potentially due to the seasonal change (winter-spring) and crop development.
- Correlations between θ and temperatures should be further studied to better understand the cooling mechanism.
- Future work includes remote sensing, wind parameters, and analyzing another crop cycle (2020-2021).

References

Desilets, D., & Zreda, M. (2006). Elevation dependence of cosmogenic 36Cl production in Hawaiian lava flows. Earth and Planetary Science Letters, 246(3–4). https://doi.org/10.1016/j.epsl.2006.03.050

Desilets, D., Zreda, M., & Ferré, T. P. A. (2010). Nature's neutron probe: Land surface hydrology at an elusive scale with cosmic rays. Water Resources Research, 46(11). https://doi.org/10.1029/2009WR008726

Duchemin, B., Fieuzal, R., Rivera, M. A., Ezzahar, J., Jarlan, L., Rodriguez, J. C., ... & Watts, C. (2015). Impact of sowing date on yield and water use efficiency of wheat analyzed through spatial modeling and FORMOSAT-2 images. Remote Sensing, 7(5), 5951-5979.

Lopes Ribeiro, F., Guevara, M., Vázquez-Lule, A., Cunha, A. P., Zeri, M., and Vargas, R.: The impact of drought on soil moisture trends across Brazilian biomes, Nat. Hazards Earth Syst. Sci., 21, 879–892, https://doi.org/10.5194/nhess-21-879-2021, 2021.

Rosolem, R., Shuttleworth, W. J., Zreda, M., Franz, T. E., Zeng, X., & Kurc, S. A. (2013). The effect of atmospheric water vapor on neutron count in the cosmic-ray soil moisture observing system. Journal of Hydrometeorology, 14(5). https://doi.org/10.1175/JHM-D-12-0120.1

Sanchez-Mejia, Z. M., & Papuga, S. A. (2014). Observations of a two-layer soil moisture influence on surface energy dynamics and planetary boundary layer characteristics in a semiarid shrubland. Water Resources Research, 50(1), 306-317.

Acknowledgement

Joint FAO/IAEA Division of Nuclear Techniques in Food and Agriculture. Coordinated Research Project (CRP) D1.20.14 Enhancing agricultural resilience and water security using Cosmic-Ray Neutron Sensor. CONACYT-CB-286494-Transporte y deposición de partículas atmosféricas en un gradiente cuenca arriba (Valle agrícola – pie de monte). The help of Miguel Rivera, Guillermo López Castro, Crhistian Silva, Javier Rivera and ITVY field managers.